

## Supporting Information for

# Amidation Induced Self-Reduction of *p*-GO with Lewis-Base Termination for All-Inorganic CsPbIBr<sub>2</sub> Perovskite Solar Cells

Jian Du,<sup>a,b</sup> Jialong Duan,<sup>a,\*</sup> Qiya Guo,<sup>a</sup> Yanyan Duan,<sup>c</sup> Xiya Yang,<sup>a</sup> Quanzhu Zhou<sup>d</sup> and Qunwei Tang<sup>a,\*</sup>

<sup>a</sup> College of Information Science and Technology, Jinan University, Guangzhou 510632, PR China;

<sup>b</sup> School of Light Industry and Chemical Engineering, Dalian Polytechnic University, Dalian 116034, China;

<sup>c</sup> State Centre for International Cooperation on Designer Low-Carbon and Environmental Material (SCICDLCEM), School of Materials Science and Engineering, Zhengzhou University Zhengzhou 450001 (P. R. China);

<sup>d</sup> BTR New Material Group Co., Ltd., Shenzhen (China).

\*Corresponding Author. Email address: duanjialong@jnu.edu.cn (J.L. Duan);  
tangqunwei@jnu.edu.cn (Q.W. Tang).

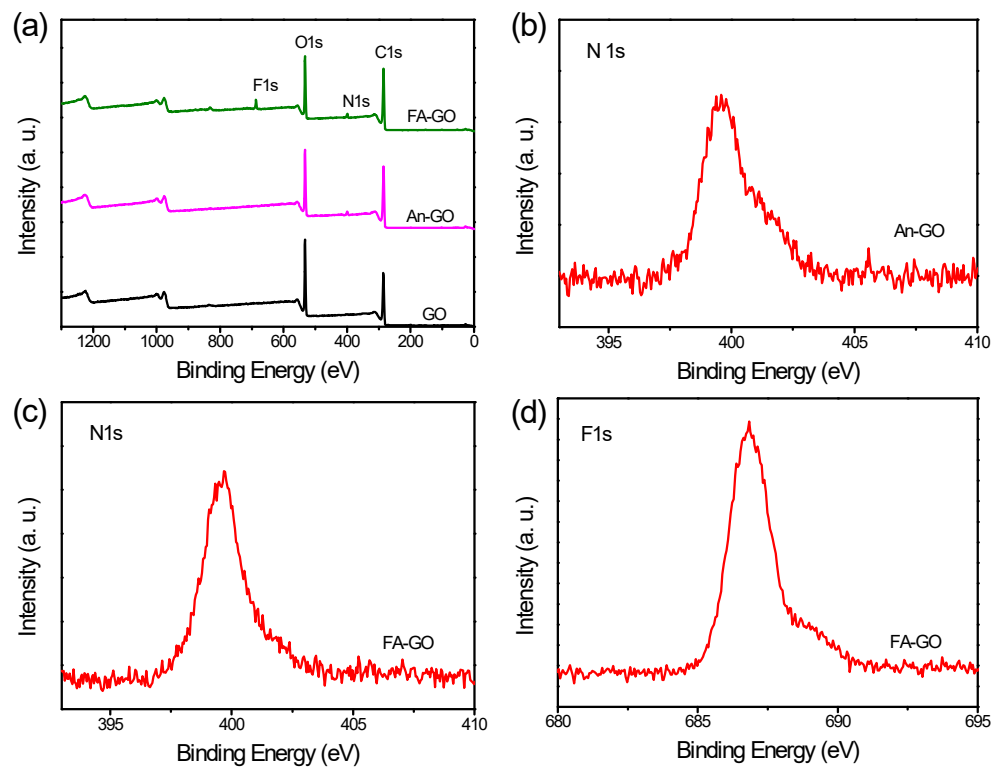


**Fig. S1** (a) XPS survey scans and high-resolution XPS spectra of N 1s and F 1s in (b) An-GO and (c-d) FA-GO.

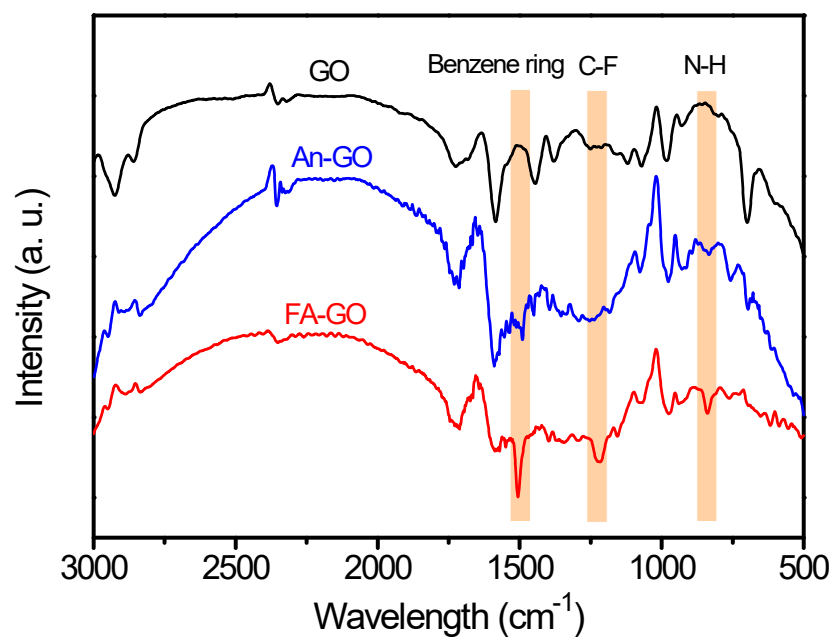


**Fig. S2** FTIR spectra of GO, An-GO and FA-GO samples.

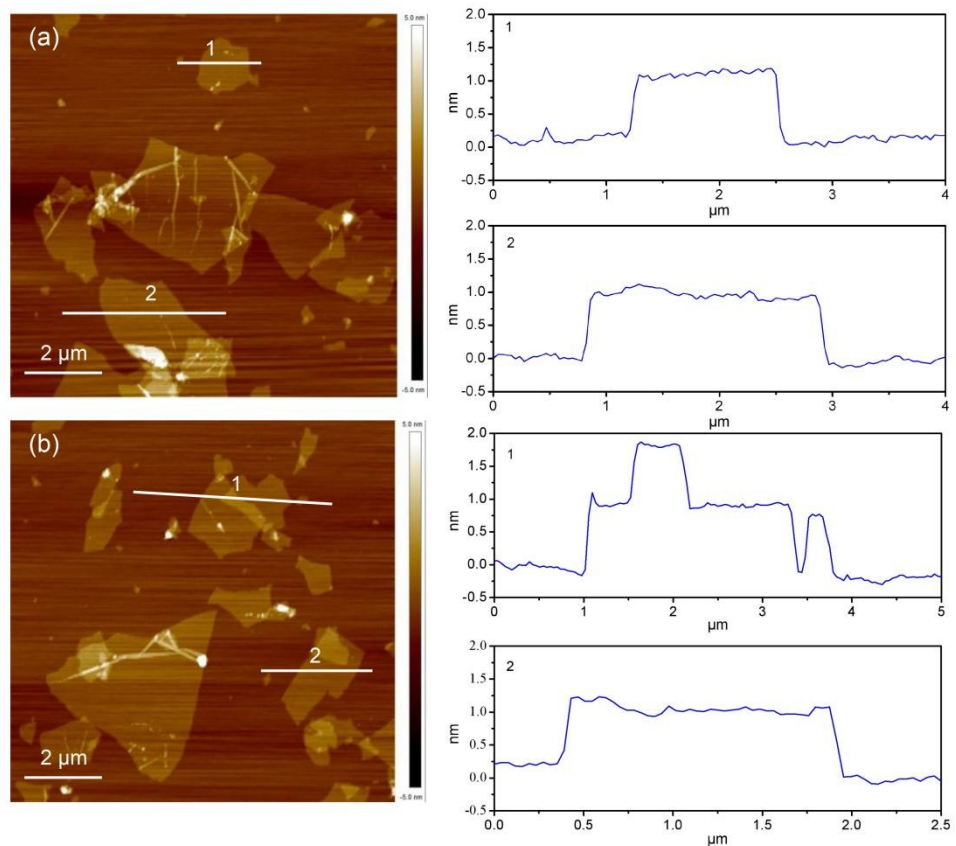


**Fig. S3** AFM images and the corresponding thickness of (a) GO and (b) FA-GO interlayers.

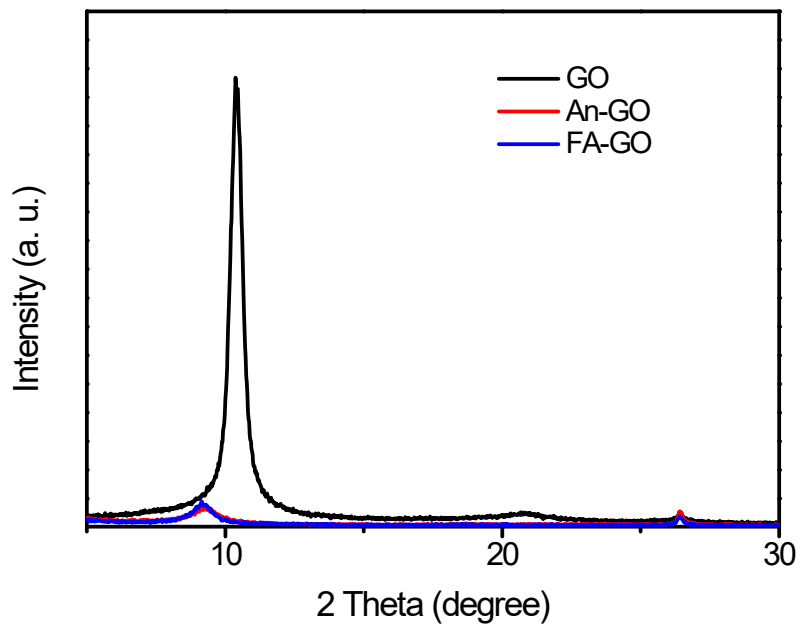


**Fig. S4** XRD patterns of GO, An-GO and FA-GO.

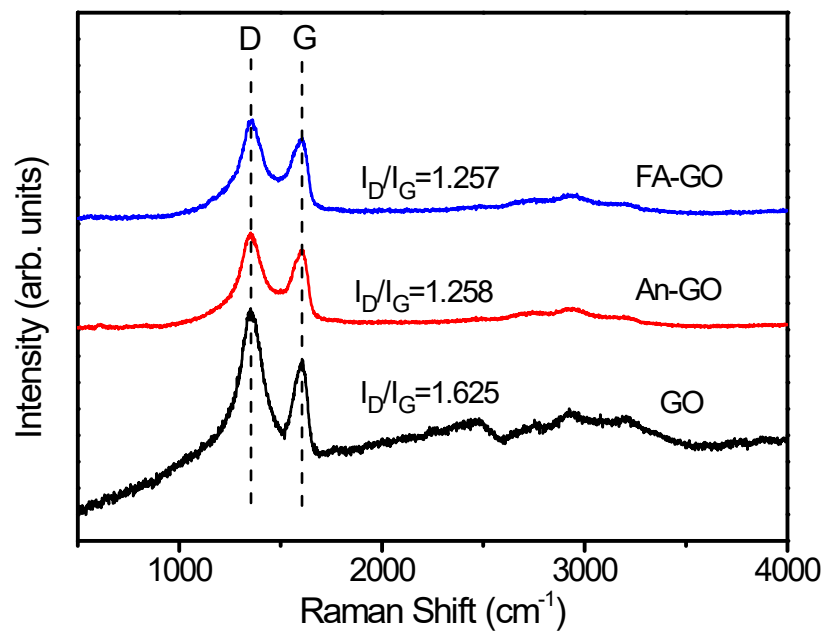


**Fig. S5** Raman spectra of GO, An-GO and FA-GO.

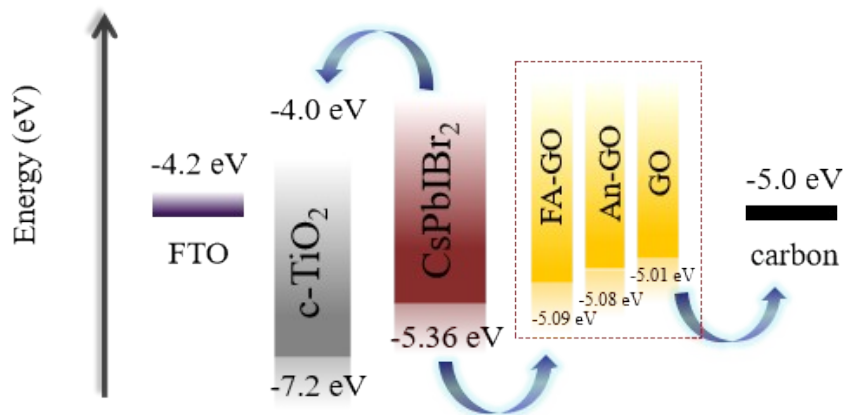


**Fig. S6** Energy-level diagram of  $\text{CsPbIBr}_2$  PSC. The energy level of  $\text{CsPbIBr}_2$  perovskite film is obtained from previous work.<sup>[S1]</sup>

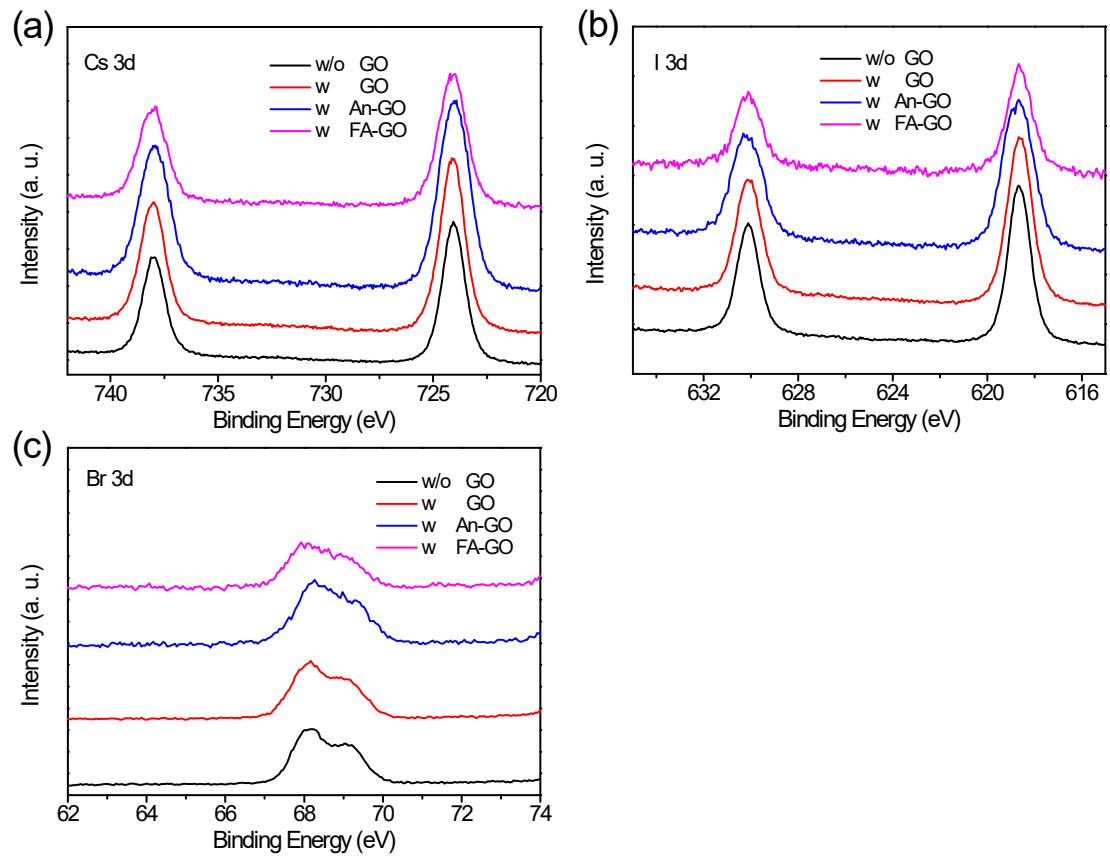


**Fig. S7** XPS spectra of Cs 3d, I 3d and Br 3d in  $\text{CsPbIBr}_2$ ,  $\text{CsPbIBr}_2 + \text{GO}$ ,  $\text{CsPbIBr}_2 + \text{An-GO}$  and  $\text{CsPbIBr}_2 + \text{FA-GO}$ .

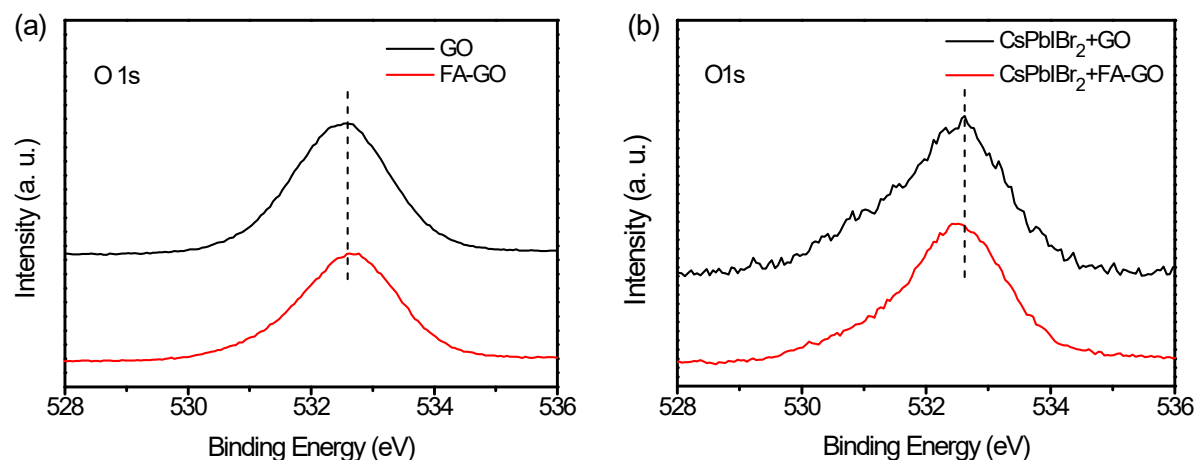


**Fig. S8** High-resolution XPS spectra of O 1s in (a) GO and FA-GO and (b) CsPbIBr<sub>2</sub> + GO and CsPbIBr<sub>2</sub> + FA-GO.

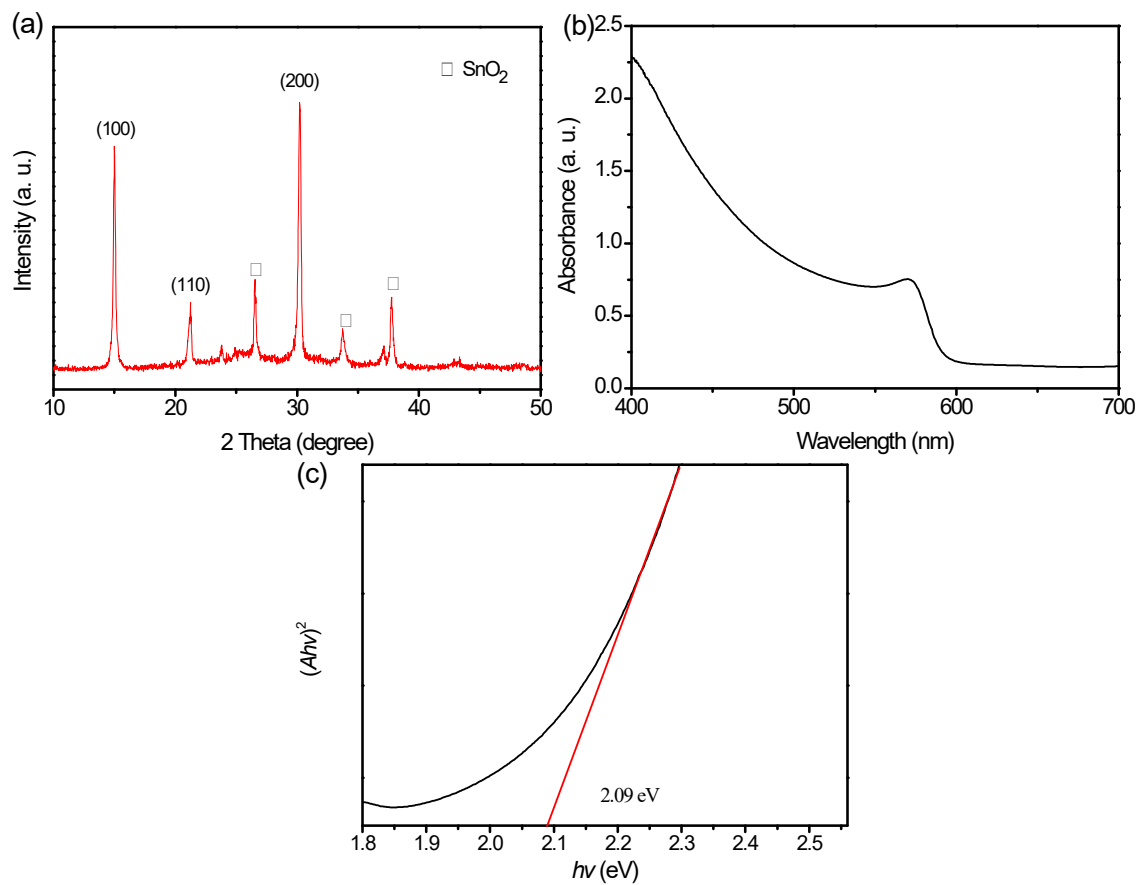


**Fig. S9** (a) XRD pattern of synthesized CsPbIBr<sub>2</sub> film on FTO/c-TiO<sub>2</sub> substrate. (b) Optical absorbance of CsPbIBr<sub>2</sub> film. (c) The bandgap of CsPbIBr<sub>2</sub> was calculated to be 2.09 eV.

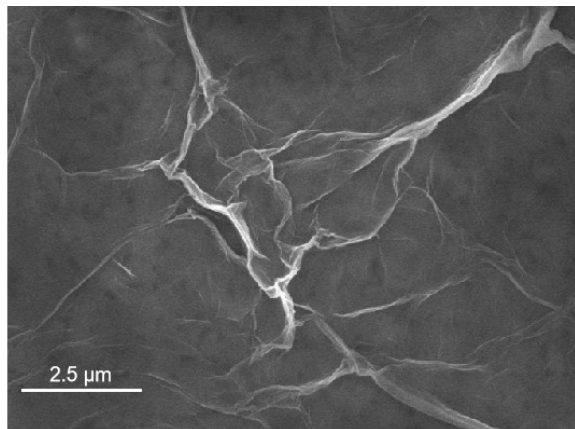


**Fig. S10** SEM image of An-GO covered perovskite film.

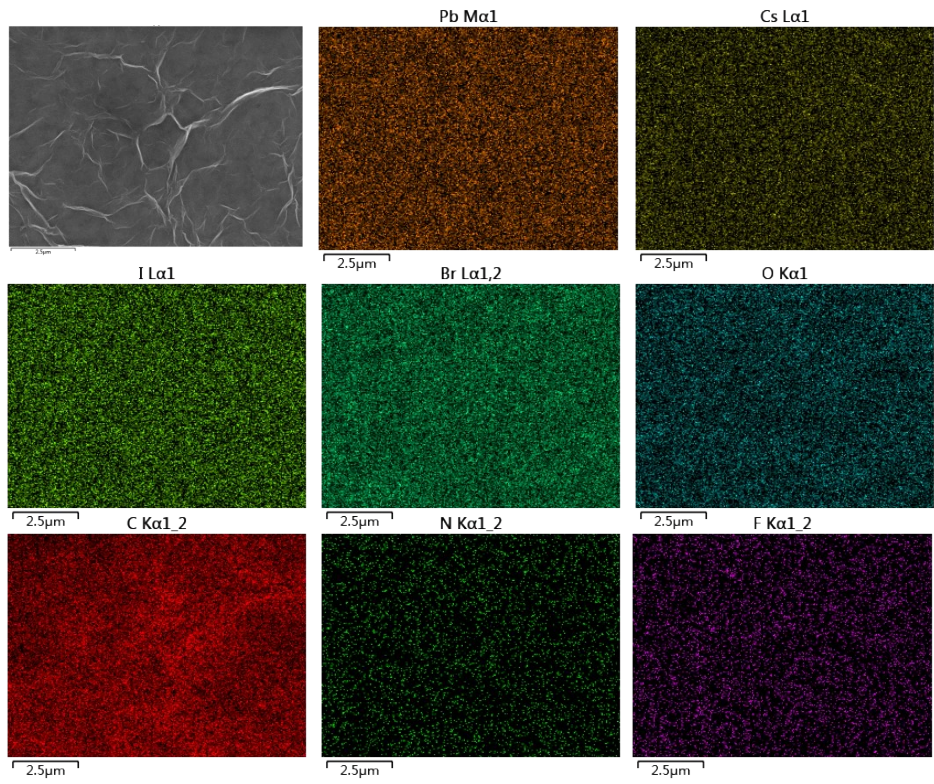


**Fig. S11** The elemental mapping images in  $\text{CsPbIBr}_2$  + FA-GO film.

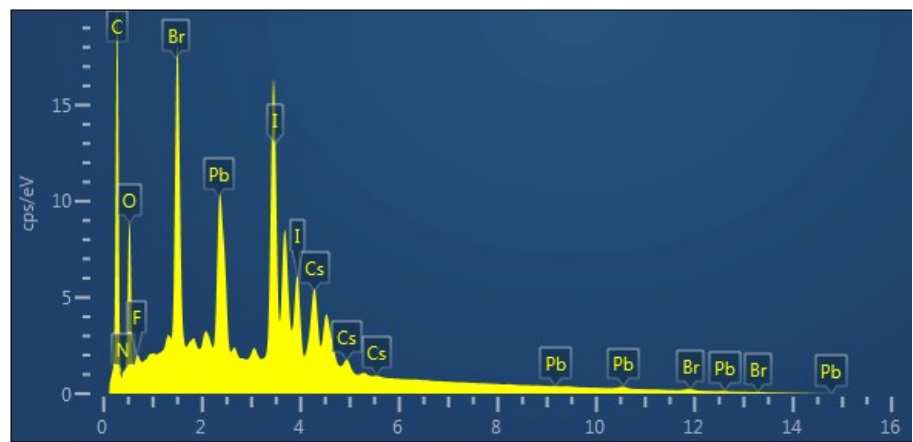


**Fig. S12** EDS spectrum of FA-GO supported on CsPbIBr<sub>2</sub> film.

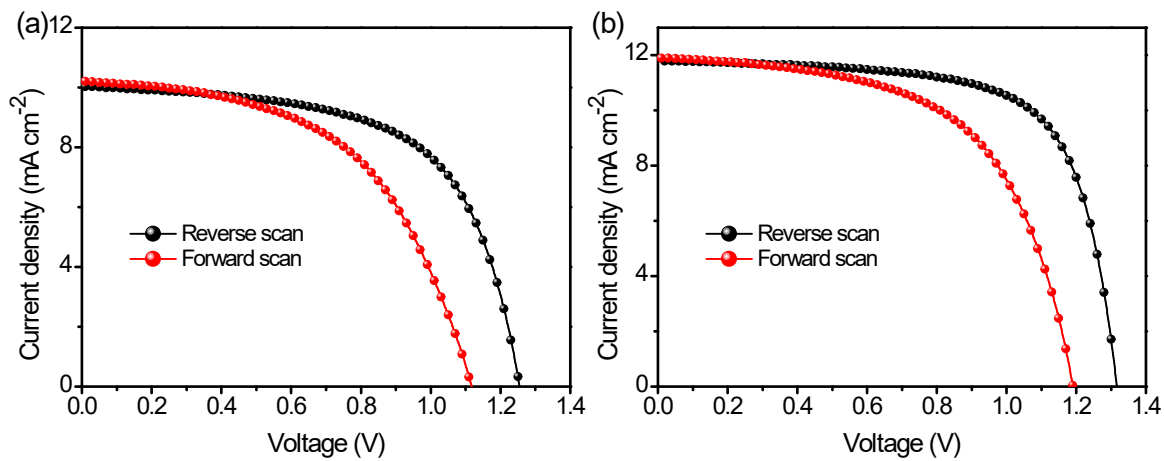


**Fig. S13**  $J$ - $V$  curves of the (a) control and (b) FA-GO tailored PSCs under forward and reverse scan directions.

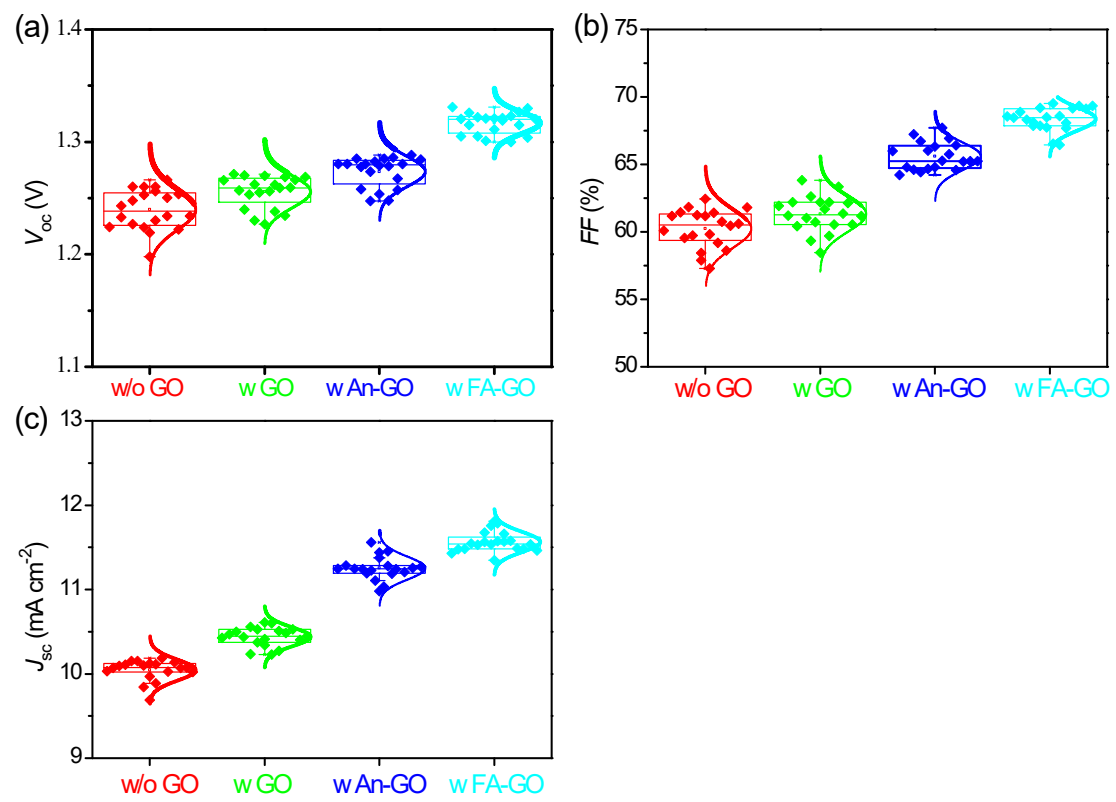


**Fig. S14** Statistical  $V_{oc}$ , FF and  $J_{sc}$  distribution of solar cells with and without treatment.

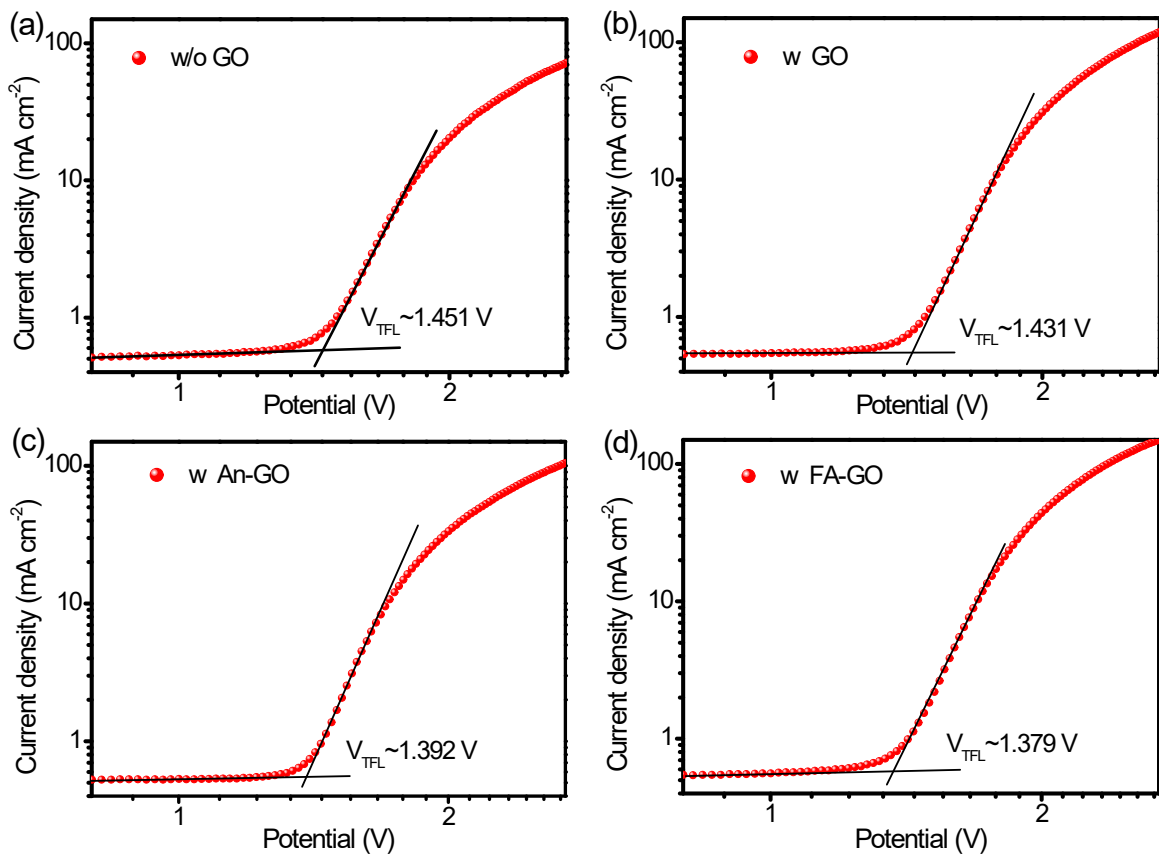


**Fig. S15** Dark current curves for the electron-only devices of perovskite films with and without GO.

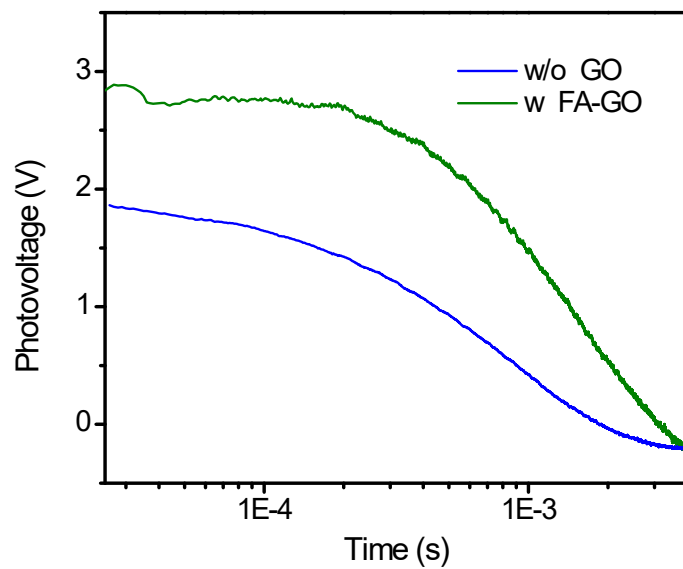


**Fig. S16** Transient photovoltage of fabricated  $\text{CsPbIBr}_2$  films with and without FA-GO.

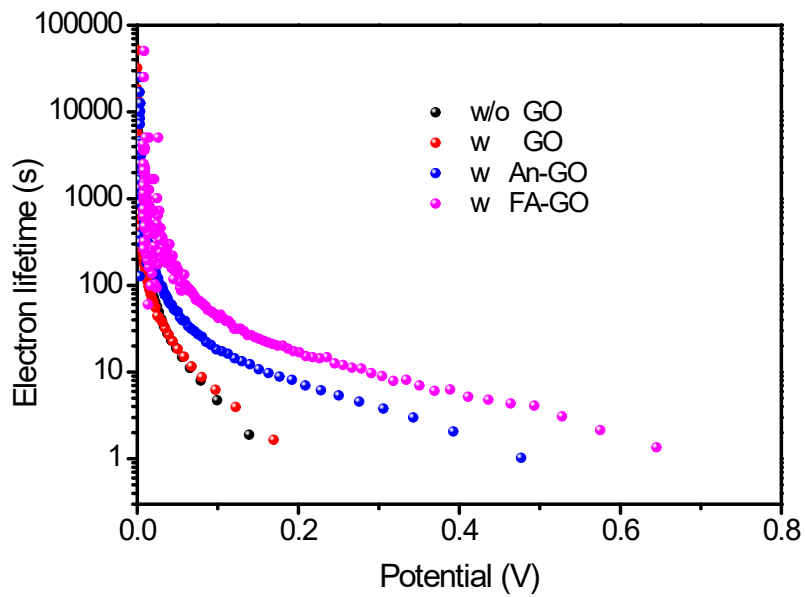


**Fig. S17** Electron lifetime calculated from  $V_{oc}$  decay curves of various devices.

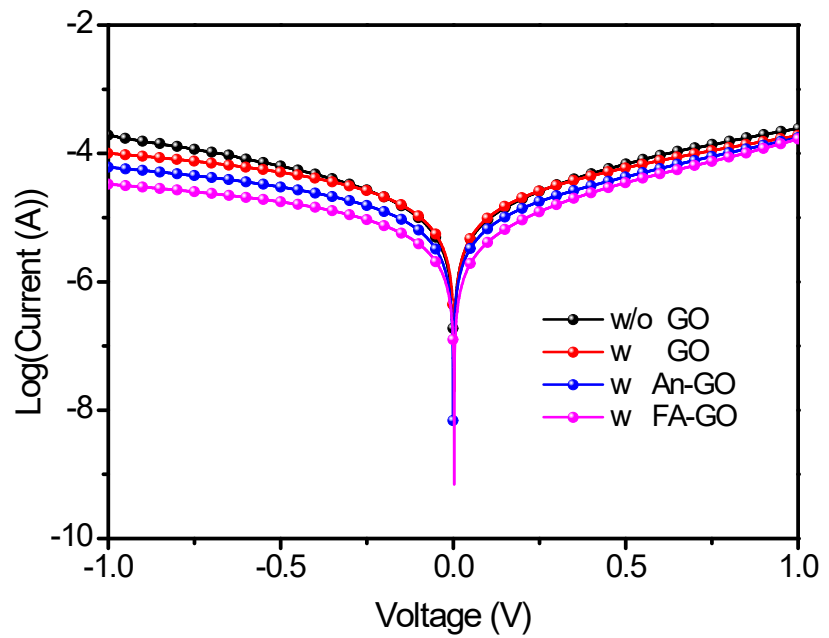


**Fig. S18** Dark  $J$ - $V$  curves of devices with and without GO.

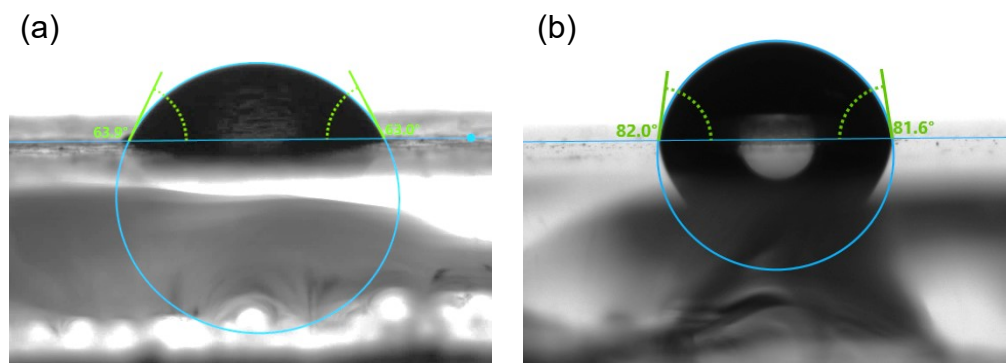


**Fig. S19** Contact angles of  $\text{CsPbIBr}_2$  and  $\text{CsPbIBr}_2/\text{FA-GO}$  films.

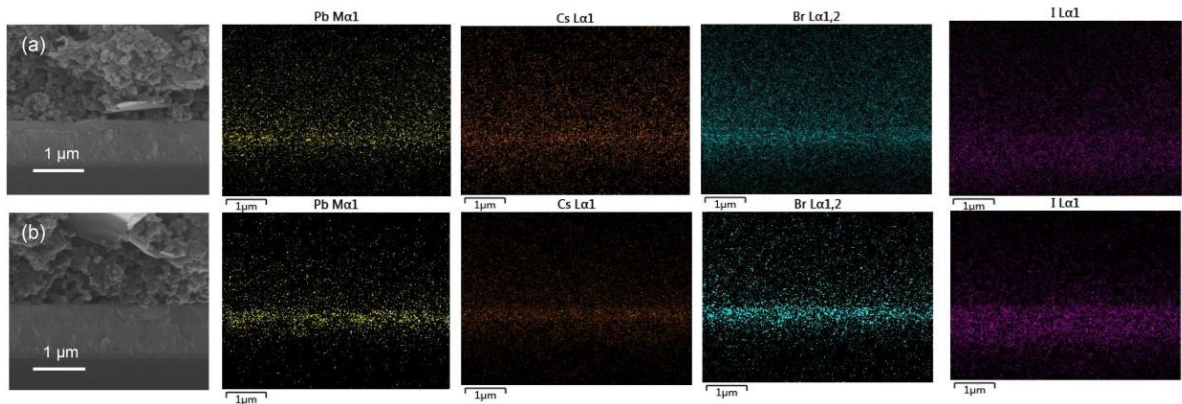


**Fig. S20** Cross-sectional SEM images and corresponding elemental mapping images of the whole devices (a) without and (b) with FA-GO after aging treatment at 150 °C for 24 h.

**Table S1.** Summary of photovoltaic parameters for state-of-the-art CsPbIBr<sub>2</sub> PSCs.

Devices	$V_{oc}$ (V)	$J_{sc}$ (mA cm <sup>-2</sup> )	FF (%)	PCE (%)	Ref.
<b>FTO/c-TiO<sub>2</sub>/CsPbIBr<sub>2</sub>/FA-GO/Carbon</b>	<b>1.318</b>	<b>11.87</b>	<b>70.84</b>	<b>11.08</b>	<b>This work</b>
FTO/TiO <sub>2</sub> /CsPbIBr <sub>2</sub> /Spiro-OMeTAD/Au	1.12	11.65	72.39	9.44	[S2]
FTO/TiO <sub>2</sub> /CsPbIBr <sub>2</sub> /carbon	1.08	10.88	64	7.52	[S3]
FTO/c-TiO <sub>2</sub> /CsPb <sub>0.99</sub> Zn <sub>0.01</sub> Br <sub>2</sub> /Spiro-OMeTAD/Ag	1.28	11.92	69	10.16	[S4]
FTO/SnO <sub>2</sub> /CsPbIBr <sub>2</sub> /carbon	1.19	9.76	57	6.79	[S5]
FTO/c-TiO <sub>2</sub> /CsPbI <sub>1+x</sub> Br <sub>2-x</sub> /carbon	1.186	12.3	75	10.94	[S6]
FTO/SnO <sub>2</sub> /CsPbIBr <sub>2</sub> -PEI/CsPbIBr <sub>2</sub> -MA/CsPbIBr <sub>2</sub> /NiO <sub>x</sub> /Ag	1.25	13.30	68	11.30	[S7]
FTO/c-TiO <sub>2</sub> /CsPbIBr <sub>2</sub> /Carbon	1.338	11.73	65	10.20	[S8]
FTO/TiO <sub>2</sub> /SmBr <sub>3</sub> /Sm-doped CsPbIBr <sub>2</sub> /Spiro-OMETAD/Au	1.17	-	-	10.88	[S9]
FTO/c-TiO <sub>2</sub> /CsBr/CsPbIBr <sub>2</sub> /Carbon	1.26	11.80	72	10.71	[S10]
ITO/Cl-TiO <sub>2</sub> /CsPbIBr <sub>2</sub> /BHJ-2/MoO <sub>3</sub> /Al	1.22	12.50	72.66	11.08	[S11]
FTO/ TiO <sub>2</sub> /CsPbIBr <sub>2</sub> /PCBM/Ag	1.25	11.63	74	10.78	[S12]
FTO/TiO <sub>2</sub> /CsPbIBr <sub>2</sub> /PCBM/Ag	1.21	11.58	69	10.48	[S13]
FTO/c-TiO <sub>2</sub> /CsPbIBr <sub>2</sub> /Spiro-OMeTAD/Au	1.10	12.03	65.40	8.65	[S14]
ITO/SnO <sub>2</sub> /bulk CsPbIBr <sub>2</sub> /QDs CsPbIBr <sub>2</sub> /Spiro-OMeTAD/Au	1.22	9.41	71.36	8.16	[S15]
ITO/SnO <sub>2</sub> /CsPbIBr <sub>2</sub> /Spiro-OMeTAD/Au	1.27	9.21	71.80	8.43	[S16]
FTO/c-TiO <sub>2</sub> /CsPbIBr <sub>2</sub> /Carbon	1.14	9.11	63	6.55	[S17]

**Table S2.** FWHM data of GO, An-GO and FA-GO.

Samples	FWHM
GO	0.48
An-GO	0.71
FA-GO	0.71

**Table S3.** TRPL decay parameters of various perovskite films.

Device	$\tau_1$	$a_1$	$\tau_2$	$a_2$	$\tau_{ave}$ (ns)
w/o GO	0.3244	24.75%	6.7256	75.25%	1.143
w GO	0.3081	38.92%	7.91688	61.08%	0.746
w An-GO	0.2719	48.88%	6.3677	51.12%	0.532
w FA-GO	0.1535	55.08%	3.7687	44.92%	0.269

## References

- [S1] Y. You, W. Tian, M. Wang, F. Cao, H. Sun, L. Li, *Adv. Mater. Interfaces* 2020, 7, 2000537.
- [S2] Z. Chen, Q. Wang, Y. Xu, R. Zhou, L. Zhang, Y. Huang, L. Hu, M. Lyu, J. Zhu, *ACS Appl. Mater. Interfaces*, 2021, DOI: 10.1021/acsami.1c02377.
- [S3] J. Liu, Q. He, J. Bi, M. Lei, W. Zhang, G. Wang, *Chem. Eng.* 2021, J. DOI: 10.1016/j.cej.2021.130324.
- [S4] Y. Long, C. Wang, X. Liu, J. Wang, S. Fu, J. Zhang, Z. Hu, Y. Zhu, *J. Mater. Chem. C*, 2021, 9, 2145.
- [S5] R. Wang, H. Zhang, S. Han, Y. Wu, Z. Hu, G. Zhang, H. Liu, Q. He, X. Zhang, *New J. Chem.*, 2021, 45, 9243.
- [S6] Z. Zhang, D. Chen, W. Zhu, J. Ma, W. Chai, D. Chen, J. Zhang, C. Zhang, Y. Hao, *Sci. China Mater.* 2021, DOI: 10.1007/s40843-020-1618-x.
- [S7] B. Gao, J. Meng, *ACS Appl. Energy Mater.* 2020, 3, 8249-8256.
- [S8] W. Zhu, Z. Zhang, D. Chen, W. Chai, D. Chen, J. Zhang, C. Zhang, Y. Hao, *Nano-Micro Lett.* 2020, 12, 87.
- [S9] W. S. Subhani, K. Wang, M. Du, X. Wang, S. Liu, *Adv. Energy Mater.* 2019, 9, 1803785.
- [S10] W. Zhu, Z. Zhang, W. Chai, Q. Zhang, D. Chen, Z. Lin, J. Chang, J. Zhang, C. Zhang, Y. Hao, *ChemSusChem* 2019, 12, 2318-2325.
- [S11] W. Chen, D. Li, S. Chen, S. Liu, Y. Shen, G. Zeng, X. Zhu, E. Zhou, L. Jiang, Y. Li, Y. Li, *Adv. Energy Mater.* 2020, 10, 2000851.
- [S12] C. Zhang, K. Wang, Y. Wang, W. S. Subhani, X. Jiang, S. Wang, H. Bao, L. Liu, L. Wan, S. Liu, *Solar RRL* 2020, 4, 2000254.

- [S13] Z. Zhang, F. He, W. Zhu, D. Chen, W. Chai, D. Chen, H. Xi, J. Zhang, C. Zhang, Y. Hao, Sustainable Energy Fuels 2020, 4, 4506-4515.
- [S14] J. Bian, Y. Wu, W. Bi, L. Liu, X. Su, B. Zhang, Energy Fuels 2020, 34, 11472-11478.
- [S15] Y. Guo, X. Yin, M. Que, J. Zhang, S. Wen, D. Liu, H. Xie, W. Que, Organic Electron. 2020, 86, 105917.
- [S16] X. Yin, Y. Guo, J. Liu, W. Que, F. Ma, K. Xu, J. Phys. Chem. Lett. 2020, 11, 7035-7041.
- [S17] W. Zhu, Q. Zhang, C. Zhang, Z. Zhang, D. Chen, Z. Lin, J. Chang, J. Zhang, Y. Hao, ACS Appl. Energy Mater. 2018, 1, 4991-4997.